Numerical simulation of incompressible flows in time-dependent domains

Alexander Lozovskiy[1] **Yuri Vassilevski**[1,2]
Maxim Olshanskii[3] **Victoria Salamatova**[1,2]
Alexander Danilov[1,2]

[1]Institute of Numerical Mathematics RAS
[2]Moscow Institute of Physics and Technology
[3]University of Houston

Germany-Russia-USA workshop on
Numerical Methods and Mathematical Modelling in
Geophysical and Biomedical sciences

June 13, 2017, Moscow

Contents

Numerical tests in 2D:

- FSI3: elastic beam in fluid
- Blood vessel with aneurysm

Numerical tests in 3D:

- Silicone filament in glycerol
- Hemodynamics in the left ventricle of human heart

Numerical scheme

$$
\begin{aligned}
&\int_{\Omega_s} \rho_s \frac{\mathbf{v}^{k+1} - \mathbf{v}^k}{\Delta t} \psi \,\mathrm{d}\mathbf{x} + \int_{\Omega_s} \mathbf{F}(\mathbf{u}^k)\mathbf{S}(\mathbf{u}^{k+1}, \mathbf{u}^k) : \nabla \psi \,\mathrm{d}\mathbf{x} \\
&+ \int_{\Omega_f} \rho_f J^{k-1} \frac{\mathbf{v}^{k+1} - \mathbf{v}^k}{\Delta t} \psi \,\mathrm{d}\mathbf{x} + \int_{\Omega_f} \rho_f J^k (\nabla \mathbf{v}^{k+1}) \mathbf{F}^{-1}(\mathbf{u}^k) \Big(\mathbf{v}^k - \frac{\mathbf{u}^k - \mathbf{u}^{k-1}}{\Delta t} \Big) \psi \,\mathrm{d}\mathbf{x} \\
&+ \int_{\Omega_f} 2\mu_f J^k \{(\nabla \mathbf{v}^{k+1}) \mathbf{F}^{-1}(\mathbf{u}^k)\}_s : \{(\nabla \psi) \mathbf{F}^{-1}(\mathbf{u}^k)\}_s \,\mathrm{d}\mathbf{x} - \int_{\Omega_f} p_f^{k+1} J^k \mathbf{F}^{-T}(\mathbf{u}^k) : \nabla \psi \,\mathrm{d}\mathbf{x} \\
&+ \int_{\Omega_f} \frac{\rho_f}{2} \frac{J^k - J^{k-1}}{\Delta t} \mathbf{v}^{k+1} \psi + \int_{\Omega_f} \frac{\rho_f}{2} \operatorname{div} \left(J^k \mathbf{F}^{-1}(\mathbf{u}^k) \left(\mathbf{v}^k - \frac{\mathbf{u}^k - \mathbf{u}^{k-1}}{\Delta t} \right) \right) \mathbf{v}^{k+1} \psi \,\mathrm{d}\mathbf{x} \\
&+ \int_{\Omega_f} \mathbf{H}(\mathbf{u}^{k+1}, \mathbf{u}^k) : \nabla \phi \,\mathrm{d}\mathbf{x} = 0 \quad \text{for all } \psi \in \mathbb{V}_h \text{ and all } \phi \in \mathbb{V}_h^0.
\end{aligned}
$$

$$
\int_{\Omega_s} \frac{\mathbf{u}^{k+1} - \mathbf{u}^k}{\Delta t} \phi \,\mathrm{d}\mathbf{x} - \int_{\Omega_s} \mathbf{v}^{k+1} \phi \,\mathrm{d}\mathbf{x} = 0 \quad \text{for all } \phi \in \mathbb{V}_h^0 \quad \text{(kinematics equation in solid)},
$$

$$
\int_{\Omega_f} J^k \nabla \mathbf{v}^{k+1} : \mathbf{F}^{-T}(\mathbf{u}^k) q \,\mathrm{d}\mathbf{x} = 0 \quad \text{for all } q \in \mathbb{Q}_h \quad \text{(incompressibility equation in fluid)}.
$$

Numerical scheme

$$\int_{\Omega_s} \rho_s \frac{\mathbf{v}^{k+1} - \mathbf{v}^k}{\Delta t} \psi \, \mathrm{d}\mathbf{x} + \int_{\Omega_s} \mathbf{F}(\mathbf{u}^k)\mathbf{S}(\mathbf{u}^{k+1}, \mathbf{u}^k) : \nabla \psi \, \mathrm{d}\mathbf{x}$$
$$+ \int_{\Omega_f} \rho_f J^{k-1} \frac{\mathbf{v}^{k+1} - \mathbf{v}^k}{\Delta t} \psi \, \mathrm{d}\mathbf{x} + \int_{\Omega_f} \rho_f J^k (\nabla \mathbf{v}^{k+1}) \mathbf{F}^{-1}(\mathbf{u}^k) \Big(\mathbf{v}^k - \frac{\mathbf{u}^k - \mathbf{u}^{k-1}}{\Delta t} \Big) \psi \, \mathrm{d}\mathbf{x}$$
$$+ \int_{\Omega_f} 2\mu_f J^k \{ (\nabla \mathbf{v}^{k+1}) \mathbf{F}^{-1}(\mathbf{u}^k) \}_s : \{ (\nabla \psi) \mathbf{F}^{-1}(\mathbf{u}^k) \}_s \, \mathrm{d}\mathbf{x} - \int_{\Omega_f} p_f^{k+1} J^k \mathbf{F}^{-T}(\mathbf{u}^k) : \nabla \psi \, \mathrm{d}\mathbf{x}$$
$$+ \int_{\Omega_f} \frac{\rho_f}{2} \frac{J^k - J^{k-1}}{\Delta t} \mathbf{v}^{k+1} \psi + \int_{\Omega_f} \frac{\rho_f}{2} \operatorname{div} \left(J^k \mathbf{F}^{-1}(\mathbf{u}^k) \left(\mathbf{v}^k - \frac{\mathbf{u}^k - \mathbf{u}^{k-1}}{\Delta t} \right) \right) \mathbf{v}^{k+1} \psi \, \mathrm{d}\mathbf{x}$$
$$+ \int_{\Omega_f} \mathbf{H}(\mathbf{u}^{k+1}, \mathbf{u}^k) : \nabla \phi \, \mathrm{d}\mathbf{x} = 0 \quad \text{for all } \psi \in \mathbb{V}_h \text{ and all } \phi \in \mathbb{V}_h^0.$$

$$\int_{\Omega_s} \frac{\mathbf{u}^{k+1} - \mathbf{u}^k}{\Delta t} \phi \, \mathrm{d}\mathbf{x} - \int_{\Omega_s} \mathbf{v}^{k+1} \phi \, \mathrm{d}\mathbf{x} = 0 \quad \text{for all } \phi \in \mathbb{V}_h^0 \quad \text{(kinematics equation in solid)},$$

$$\int_{\Omega_f} J^k \nabla \mathbf{v}^{k+1} : \mathbf{F}^{-T}(\mathbf{u}^k) q \, \mathrm{d}\mathbf{x} = 0 \quad \text{for all } q \in \mathbb{Q}_h \quad \text{(incompressibility equation in fluid)}.$$

Follows from $\frac{\partial J}{\partial t} + \operatorname{div}(J\mathbf{F}^{-1}(\mathbf{v} - \frac{\partial \mathbf{u}}{\partial t})) = 0$ in Ω_f.

Examples of displacement extension:

- Linear elasticity:

$$-\int_{\Omega_f} (2\mu_m \{\nabla \mathbf{u}^{k+1}\}_s : \nabla \phi + \lambda_m \mathrm{div}\, \mathbf{u}^{k+1} \mathrm{div}\, \phi) \, \mathrm{d}\mathbf{x}$$

- Harmonic:

$$-\int_{\Omega_f} \nabla \mathbf{u}^{k+1} \nabla \phi \, \mathrm{d}\mathbf{x}$$

- Heat:

$$\int_{\Omega_f} \frac{\mathbf{u}^{k+1} - \mathbf{u}^k}{\Delta t} \phi \, \mathrm{d}\mathbf{x} - \alpha \int_{\Omega_f} \nabla \mathbf{u}^{k+1} \nabla \phi \, \mathrm{d}\mathbf{x}$$

Validation in 2D: FSI3 benchmark problem

S. Turek and J. Hron. Proposal for numerical benchmarking of fluid-structure interaction between an elastic object and laminar incompressible flow. In: *Fluid-structure interaction*, Springer Berlin Heidelberg, 371–385, 2006.

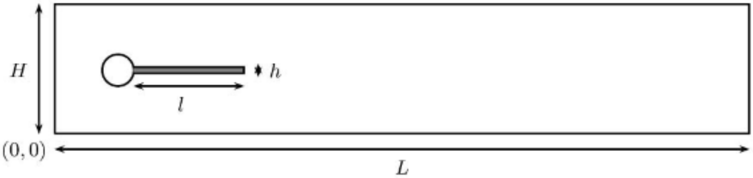

$$L = 2.5,\ H = 0.41,\ l = 0.35,\ h = 0.02.$$

- fluid: 2D transient Navier-Stokes, $\rho_f = 1000$, $\mu_f = 1$
- stick: SVK constitutive relation, $\rho_s = 1000$, $\lambda_s = 4\mu_s = 8 \cdot 10^6$
- outflow: “do-nothing”
- rigid walls: no-slip condition

Validation in 2D: FSI3 benchmark problem

S. Turek and J. Hron. Proposal for numerical benchmarking of fluid-structure interaction between an elastic object and laminar incompressible flow. In: *Fluid-structure interaction*, Springer Berlin Heidelberg, 371–385, 2006.

- inflow: parabolic profile

$$v_x(0,y,t) = \frac{12}{0.1681} v(t) y(H-y), \quad y \in [0,H],$$

where

$$v(t) = \begin{cases} \frac{1}{2}\left(1 - \cos\left(\frac{\pi t}{2}\right)\right) & \text{for } t < 2, \\ 1 & \text{for } t \geq 2. \end{cases}$$

- Linear elasticity extension operator for displacement in Ω_f
- Taylor-Hood element $(P_2 + P_1)$ for fluid and P_2 for solid.
- Grad-Div stabilization for fluid.
- Simulations were run using BDF with time step $\Delta t = 10^{-3}$ until $T = 8$.
- UMFPACK solver for linear systems

Validation in 2D: FSI3 benchmark problem

S. Turek and J. Hron. Proposal for numerical benchmarking of fluid-structure interaction between an elastic object and laminar incompressible flow. In: *Fluid-structure interaction*, Springer Berlin Heidelberg, 371–385, 2006.

Fortran open source software `Ani2D`, `http://sf.net/p/ani2d/`:

	# of cells in Ω_f	# of cells in Ω_s	# of DOFs
Mesh 1	8652	162	76557
Mesh 2	17540	334	154242
Mesh 3	35545	658	310997

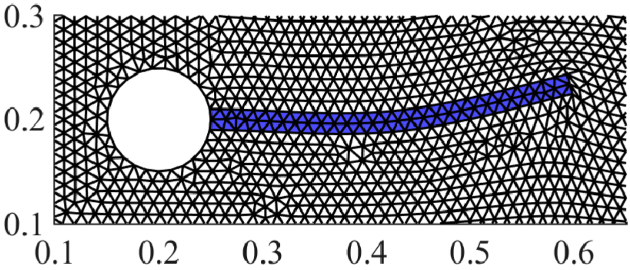

Validation in 2D: FSI3 benchmark problem

S. Turek and J. Hron. Proposal for numerical benchmarking of fluid-structure interaction between an elastic object and laminar incompressible flow. In: *Fluid-structure interaction*, Springer Berlin Heidelberg, 371–385, 2006.

Table: computed statistics for FSI3 test for the time interval [7,8]

Mesh/method	$u_x \cdot 10^3$	$u_y \cdot 10^3$	F_D	F_L
1	-2.8 ± 2.6	1.5 ± 34.3	432.9 ± 22.3	0.98 ± 152.1
2	-3.0 ± 2.8	1.4 ± 35.9	453.8 ± 26.8	2.6 ± 154.0
3	$\mathbf{-3.0 \pm 2.9}$	$\mathbf{1.4 \pm 36.1}$	$\mathbf{458.0 \pm 27.6}$	$\mathbf{3.0 \pm 154.5}$
Turek, S. et al	$[-3.04, -2.84]$ $\pm[2.67, 2.87]$	$[1.28, 1.55]$ $\pm[34.61, 46.63]$	$[452.4, 474.9]$ $\pm[26.19, 36.63]$	$[1.81, 3.86]$ $\pm[152.7, 165.9]$
Liu, J.	-2.91 ± 2.74	1.46 ± 35.2	460.3 ± 27.67	2.41 ± 157

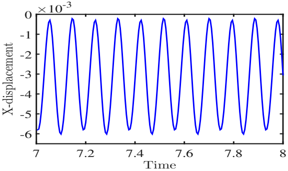

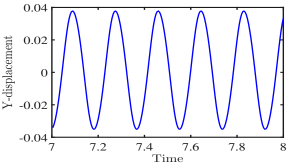

Validation in 2D: FSI3 benchmark problem

S. Turek and J. Hron. Proposal for numerical benchmarking of fluid-structure interaction between an elastic object and laminar incompressible flow. In: *Fluid-structure interaction*, Springer Berlin Heidelberg, 371–385, 2006.

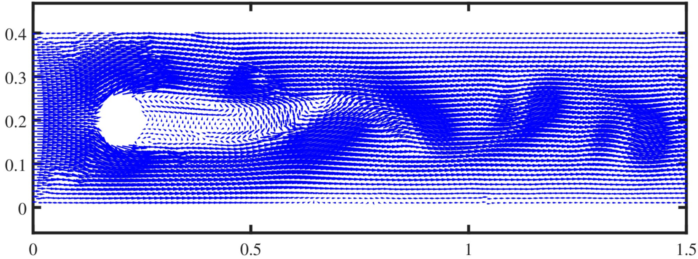

Displacement extension in fluid domain:

- Harmonic $\rightarrow$ mesh tangling
- Linear elasticity with $\mu_m = \mu_s$ and $\lambda_m = \lambda_s$ $\rightarrow$ mesh tangling
- Linear elasticity with $\mu_m = 20\mu_s$ and $\lambda_m = 20\lambda_s$ for adjacent to the beam elements $\rightarrow$ OK

2D test: blood vessel with aneurysm

S. Turek et al. Numerical simulation and benchmarking of a monolithic multigrid solver for fluid-structure interaction problems with application to hemodynamics. In: *Fluid Structure Interaction II*, Springer Berlin Heidelberg, 193–220, 2010.

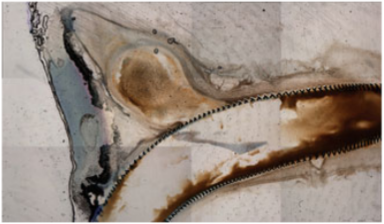

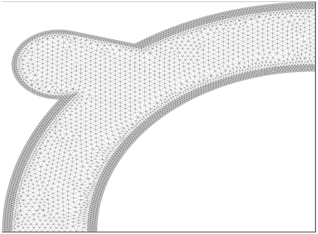

- Showing reliability of the semi-implicit scheme for hemodynamic applications
- Investigating sensitivity to compressibility of the vessel material: measuring wall shear stress(WSS) since it serves as a good indicator for the risk of aneurysm rupture

2D test: blood vessel with aneurysm

S. Turek et al. Numerical simulation and benchmarking of a monolithic multigrid solver for fluid-structure interaction problems with application to hemodynamics. In: *Fluid Structure Interaction II*, Springer Berlin Heidelberg, 193–220, 2010.

- Material properties:

ρ_s	μ_s	ρ_f	μ_f
$1.12 \cdot 10^3$ kg/m^3	270000 Pa	$1.035 \cdot 10^3$ kg/m^3	$3.4983 \cdot 10^{-3}$ Pa $\cdot$ s

- Weakly compressible neo-Hookean model:

$$\boldsymbol{\sigma}_s = \frac{\mu_s}{J^2}\left(\mathbf{F}\mathbf{F}^T - \frac{1}{2}\mathrm{tr}\,(\mathbf{F}\mathbf{F}^T)\mathbf{I}\right) + \left(\lambda_s + \frac{2\mu_s}{3}\right)(J-1)\mathbf{I}, \quad \lambda_s \to \infty$$

  Extrapolation is used in the model to retain semi-implicitness

- Pulsatile parabolic inflow profile:

$$v_1(0, y, t) = -50(8-y)(y-6)(1 + 0.75\sin(2\pi t)), \quad 6 \le y \le 8.$$

- λ_s takes on values 10^4, 10^6, 10^8 kPa, i.e. Poisson's ratio $\nu \to 0.5$.
- Time step $\Delta t = 10^{-3}$ s until $T = 3$ s.
- Elasticity based displacement extension with $\mu_m = \mu_s$, $\lambda_m = 4\lambda_s$.

2D test: blood vessel with aneurysm

S. Turek et al. Numerical simulation and benchmarking of a monolithic multigrid solver for fluid-structure interaction problems with application to hemodynamics. In: *Fluid Structure Interaction II*, Springer Berlin Heidelberg, 193–220, 2010.

Global pressure made of p_s and p_f is **not** continuous along the interface Γ_{fs} in general!

One variable for pressure : $\left[\begin{array}{c|c|c} \text{kinematics: } \mathbf{u} & \text{kinematics: } \mathbf{v} & \mathbf{0} \\ \hline \text{dynamics: } \mathbf{u} & \text{dynamics: } \mathbf{v} & p \\ \hline \mathbf{0} & \text{incompressibility} & \mathbf{0} \end{array}\right]$

Two variables for pressure : $\left[\begin{array}{c|c|c|c} \text{kinematics: } \mathbf{u} & \text{kinematics: } \mathbf{v} & \mathbf{0} & \mathbf{0} \\ \hline \text{dynamics: } \mathbf{u} & \text{dynamics: } \mathbf{v} & p_f & p_s \\ \hline \mathbf{0} & \text{incompressibility} & \mathbf{0} & \mathbf{0} \\ \hline \mathbf{0} & \text{incompressibility} & \mathbf{0} & \mathbf{0} \end{array}\right]$

2D test: blood vessel with aneurysm

S. Turek et al. Numerical simulation and benchmarking of a monolithic multigrid solver for fluid-structure interaction problems with application to hemodynamics. In: *Fluid Structure Interaction II*, Springer Berlin Heidelberg, 193–220, 2010.

WSS for weakly incompressible and fully incompressible cases, with unified and disconntected pressure:

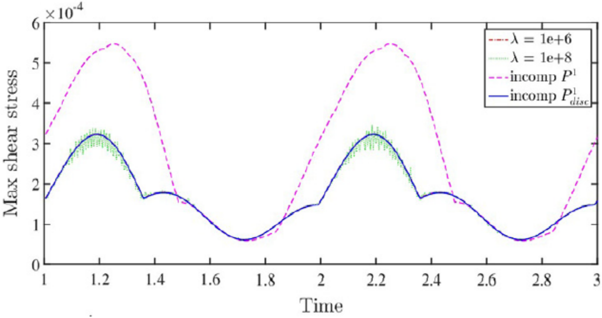

2D test: blood vessel with aneurysm

S. Turek et al. Numerical simulation and benchmarking of a monolithic multigrid solver for fluid-structure interaction problems with application to hemodynamics. In: *Fluid Structure Interaction II*, Springer Berlin Heidelberg, 193–220, 2010.

Oscillations for unified pressure decrease with mesh refinement:

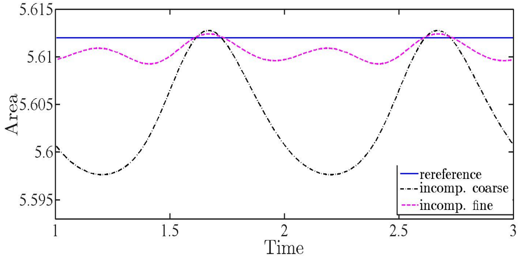

Best choices (area of wall, WSS): Neo-Hookean compressible with moderate λ_s and incompressible with disconnected pressures. The first one has fewer DOFs.

3D: silicone filament in glycerol

Benchmark challenge for CMBE 2015, Paris

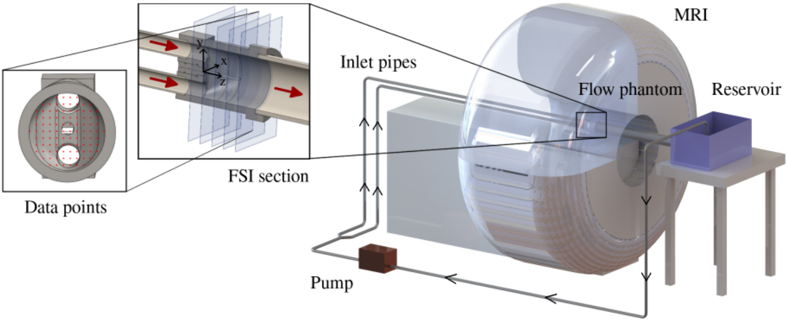

Image from A. Hessenthaler et al. Experiment for validation of fluid-structure interaction models and algorithms. *Int. J. for Numer. Meth. Biomed. Engng.*, 2016

3D: silicone filament in glycerol

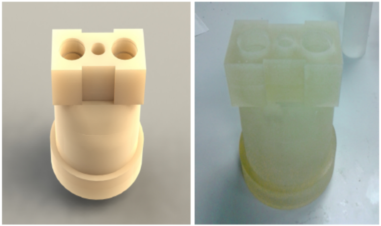

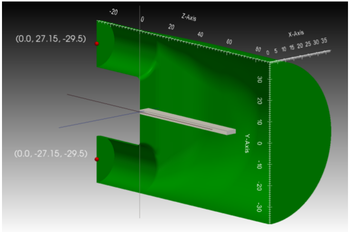

Meshed volume: original and extended domains.

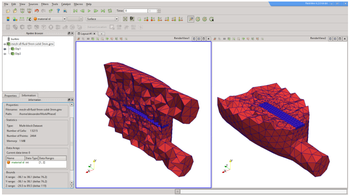

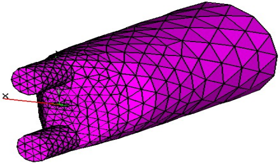

3D: silicone filament in glycerol

SVK material

M. Landajuela et al. Coupling schemes for the FSI forward prediction challenge: comparative study and validation. In: *Int. J. for Numer. Meth. in Biomed. Engng.*, 2016.

- $\rho_s = 1.063 \cdot 10^{-3}$ g mm^{-3}, $\lambda_s = 140.12$ kg s^{-2}mm^{-1}, $\mu_s = 82.2$ kg s^{-2}mm^{-1}, gravity **not** neglected!
- Two inflow regimes:

	Phase I	Phase II
velocity	stationary	pulsatile
ρ_f	$1.1633 \cdot 10^{-3}$ g mm^3	$1.164 \cdot 10^{-3}$ g mm^{-3}
μ_f	$12.5 \cdot 10^{-3}$ g mm^{-1}s^{-1}	$13.37 \cdot 10^{-3}$ g mm^{-1}s^{-1}

- Inflow velocities for one cycle of frequency 1/6 Hz for phase II:

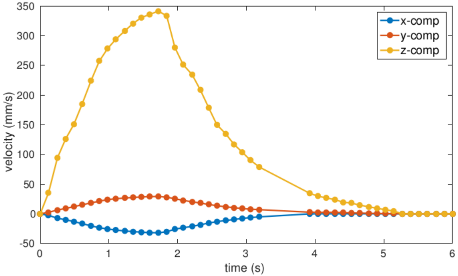

3D: silicone filament in glycerol

SVK material

M. Landajuela et al. Coupling schemes for the FSI forward prediction challenge: comparative study and validation. In: *Int. J. for Numer. Meth. in Biomed. Engng.*, 2016.

Fortran open source software `Ani3D`, `http://sf.net/p/ani3d/`

- Simulation was run with $\Delta t = 10^{-2}$ s.
- The filament is lighter than the fluid and deflects upward
- Linear elasticity model is used for the **update** of the displacement extension in Ω_f! The PDE model is non-linear due to mapping to the reference domain. The Lame parameters are heterogeneous, i.e. element-volume dependent:

$$\lambda_m = 16\mu_m = 16\frac{\mu_s}{v_e^{1.2}}.$$

- Multi-frontal massively parallel sparse direct solver (MUMPS) to solve the linear system at every time step.

3D: silicone filament in glycerol

SVK material

M. Landajuela et al. Coupling schemes for the FSI forward prediction challenge: comparative study and validation. In: *Int. J. for Numer. Meth. in Biomed. Engng.*, 2016.

	# of cells in Ω_f	# of cells in Ω_s	# of DOFs
Mesh 1	28712	733	259914
Mesh 2	51496	733	459984

Deflection due to buoyancy force:

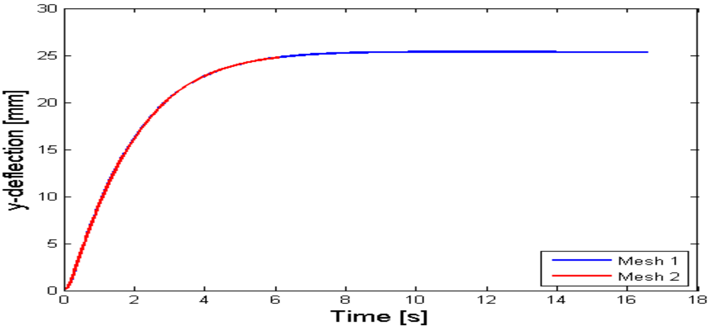

3D: silicone filament in glycerol

SVK material

M. Landajuela et al. Coupling schemes for the FSI forward prediction challenge: comparative study and validation. In: *Int. J. for Numer. Meth. in Biomed. Engng.*, 2016.

Phase I:

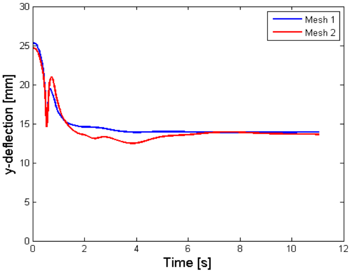

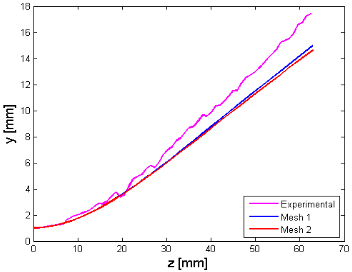

3D: silicone filament in glycerol

SVK material

M. Landajuela et al. Coupling schemes for the FSI forward prediction challenge: comparative study and validation. In: *Int. J. for Numer. Meth. in Biomed. Engng.*, 2016.

Phase II:

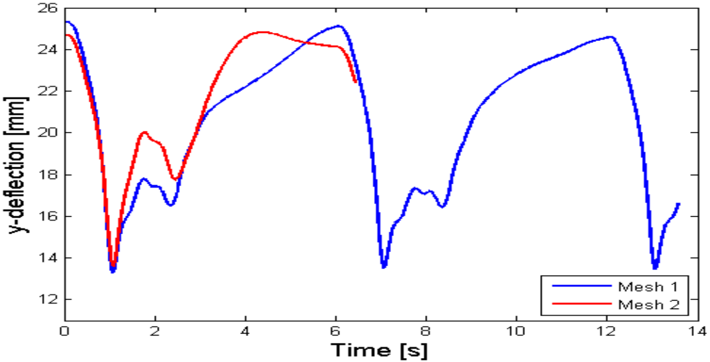

3D: left ventricle of a human heart

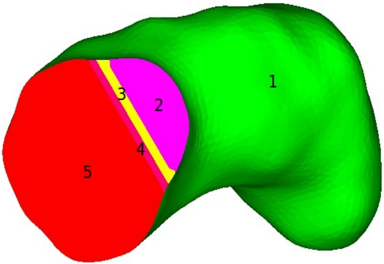

Figure: Left ventricle

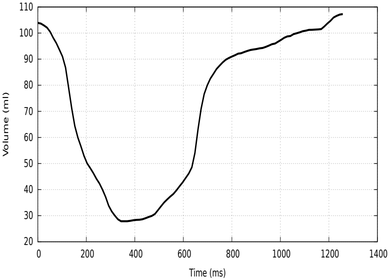

Figure: Ventricle volume

The law of motion for the ventricle walls is known thanks to ceCT scans $\rightarrow$ 100 mesh files with time gap 0.0127 s $\rightarrow$ $\mathbf{u}$ given as input $\rightarrow$ FSI reduced to NSE in a moving domain.

- 2 - aortic valve (outflow).
- 5 - mitral valve (inflow).

3D: left ventricle of a human heart

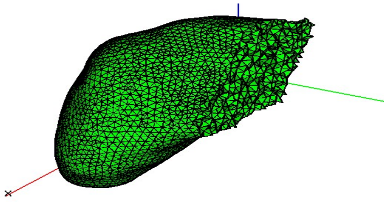

- Quasi-uniform mesh: 14033 vertices, 69257 elements, 88150 edges.
- Boundary conditions: Dirichlet $\mathbf{v} = \frac{\partial \mathbf{u}}{\partial t}$ except:
  - Do-nothing on aortal valve during systole
  - Do-nothing on mitral valve during diastole
- Time step 0.0127 s is too large! $\implies$ refined to $\Delta t = 0.0127/20$ s $\implies$ Cubic-splined $\mathbf{u}$.
- Blood parameters: $\rho_f = 10^3$ kg/m^3, $\mu_f = 4 \cdot 10^{-3}$ Pa $\cdot$s.

3D: left ventricle of a human heart

DNS resulted in convective instability during sharp deformation phases.
Physics-changing workaround: 10 x viscosity and milder wall motion.

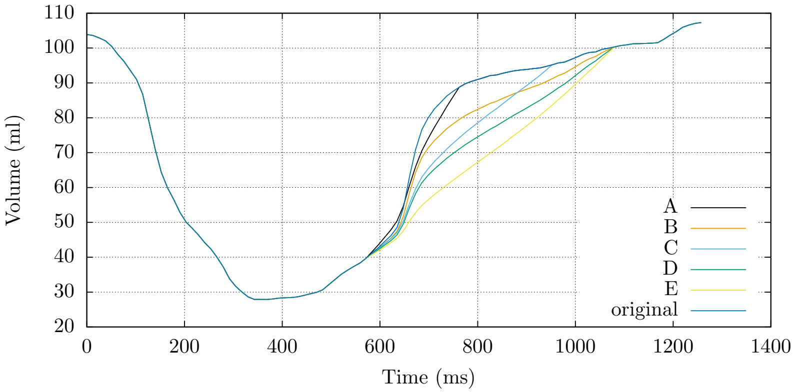

3D: left ventricle of a human heart

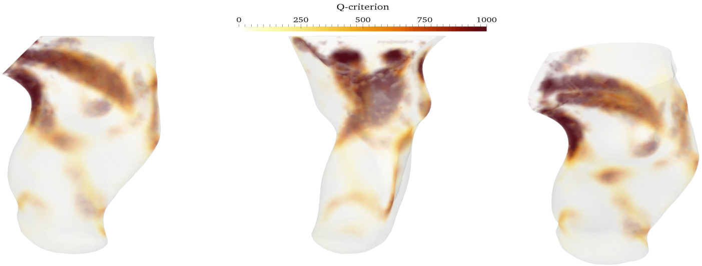

(a) (b) (c)

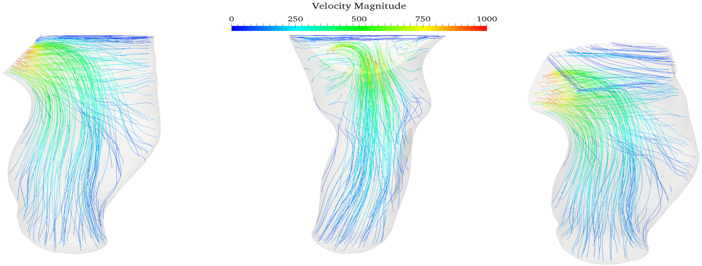

(a) (b) (c)

3D: left ventricle of a human heart

Alternative using LES: simple Smagorinsky-alike filtered model.
Scheme(in the current configuration):

$$\mathbf{z}^{k-1} := \mathbf{w}^{k-1} - \frac{\mathbf{u}^k - \mathbf{u}^{k-1}}{\Delta t},$$

$$\int_{\Omega(t^{k-1})} \frac{\mathbf{w}^k - \mathbf{w}^{k-1}}{\Delta t} \cdot \boldsymbol{\psi}\, \mathrm{d}\mathbf{x} + \int_{\Omega(t^{k-1})} \nabla \mathbf{w}^k \mathbf{z}^{k-1} \cdot \boldsymbol{\psi}\, \mathrm{d}\mathbf{x}$$
$$- \int_{\Omega(t^{k-1})} s^k \operatorname{div} \boldsymbol{\psi}\, \mathrm{d}\mathbf{x} + \int_{\Omega(t^{k-1})} q \operatorname{div} \mathbf{w}^k\, \mathrm{d}\mathbf{x} + \int_{\Omega(t^{k-1})} 2\nu \{\nabla \mathbf{w}^k\}_s : \nabla \boldsymbol{\psi}\, \mathrm{d}\mathbf{x} +$$
$$\sum_e \int_{\Omega_e(t^{k-1})} 2\nu_T^{k-1} \{\nabla \mathbf{w}^k\}_s : \nabla \boldsymbol{\psi}\, \mathrm{d}\mathbf{x} = 0,$$

where

$$\nu_T^{k-1} = 0.04 h_e^2 \sqrt{2\{\nabla \mathbf{z}^{k-1}\}_s : \nabla \mathbf{z}^{k-1}}.$$

Worked for the entire cardiac cycle with the original viscosity and mesh!

3D: left ventricle of a human heart

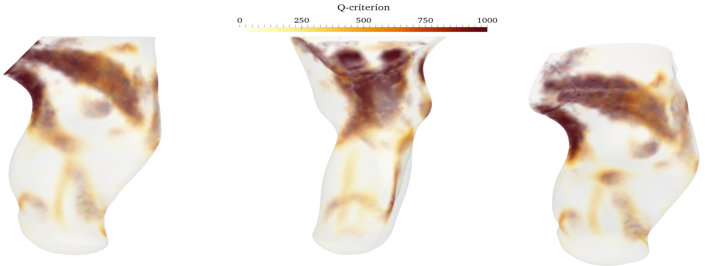

(a) (b) (c)

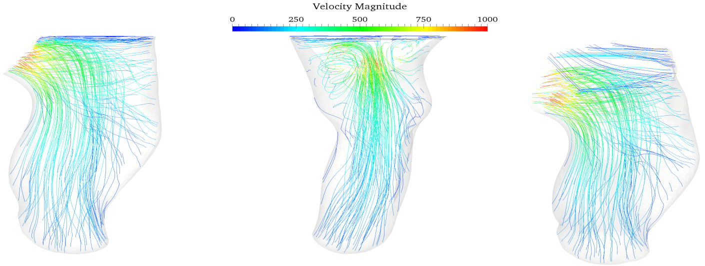

(a) (b) (c)

Thanks for your attention!